ANALYSIS OF THE DETECTABILITY OF LAVA FLOW FORMATIONS ON VENUS BY SUBSURFACE RADAR SOUNDING SIMULATIONS

Ludovica Maria Beati, Marco Cortellazzi, Lorenzo Bruzzone

Department of Information Engineering and Computer Science, University of Trento, Italy

ABSTRACT

Radar Sounder (RS) instruments are crucial for planetary exploration, as they can penetrate surfaces and reveal subsurface geological features. The next ESA's EnVision mission, scheduled to be launched in 2031 for the exploration of Venus, will carry the Subsurface Radar Sounder (SRS) to profile the surface crust at low frequencies and increase our understanding of the geological history of Venus. In this context, data simulators play a key role in the prediction and interpretation of instrument-specific results, modelling different geoelectrical and morphological features in the analysed scenario. In this paper, we present a study of the SRS's ability to detect the subsurface structures of lava flows which are one of the targets of interest. This is accomplished by examining morphological features such as their thickness and their geoelectrical properties through simulations. The results show that SRS has favourable conditions to achieve the scientific goals in detecting lava flow subsurface structures.

Index Terms— radar simulations, radar sounder, Venus, subsurface, EnVision, SRS

1. INTRODUCTION

Radar Sounder (RS) are fundamental for characterizing the subsurface of celestial bodies. Using low frequencies and nadir configurations, they conduct non-invasive surveys of subsurface targets. The emitted electromagnetic waves penetrate surfaces up to hundreds of metres deep, depending on the dielectric properties of the target. When encountering interfaces, such as dielectric discontinuities, these waves are reflected back toward the instrument. The received signals are collected in radargrams, that show a vertical profile of the target scenario. From the analysis of these radargrams one can derive information about the target's structures. However, complex geological and geophysical features, combined with the ambiguity of the signals, make RS data analysis challenging, especially with a limited prior knowledge on the considered scenario. In this context, simulations are fundamental for data interpretation, subsurface scenario understanding, and radar parameter selections, providing insight into the instrument's capabilities and constraints under specific assumptions. Planetary radar sounders have played a crucial role in advancing our understanding of the solar system's planet formation and evolution. In past years, they have become relevant components of various planetary missions for targets as the Moon [1] [2] and Mars [3] [4]. More recently, the ESA's JUICE mission [5], launched in April 2023 with RIME [6] on board, aims to profile the subsurface of the icy moons of the Jovian system, while NASA's Europa Clipper mission, scheduled for 2024, with REASON [7] on board, has the objective to explore the subsurface of Jupiter's moon Europa. Following this legacy of planetary RS, the Subsurface Radar Sounder (SRS) [8] onboard ESA's EnVision mission directed to Venus will be launched in 2031. SRS, the first RS on board a spacecraft to Venus, is designed as a nadir-looking radar operating in a single frequency band centered at $9\ MHz$ with a bandwidth of $5\ MHz$. These specific characteristics have been selected to meet mission requirements, ensuring the capability to achieve a penetration depth ranging from a few ten meters to a few hundred meters, coupled with a vertical resolution of approximately $20\ m$ for targets possessing a real permittivity equal to 6. SRS aims to collect fundamental data on the geology of the subsurface. The instrument will help provide valuable information of the origin of target of interest, such as the lava flows, by mapping structure and dielectric interfaces. In addition, SRS will contribute to provide surface information, including roughness, composition and permittivity properties, enhancing the understanding of surface features.

Electromagnetic simulators have been employed to simulate RS data from geoelectrical models representing subsurface scenarios, supporting planetary exploration missions. However, limited studies currently exist on subsurface response analysis of Venusian targets, especially using detailed radar response simulations [9], [10], as Venus's composition properties are largely unknown. Volcanic eruptions are pivotal resurfacing events on Venus. EnVision aims to characterize lava flows to understand their nature and thickness, with SRS playing a crucial role in examining the base of lava flows.

In this paper, we comprehensively analyze SRS's ability to detect and differentiate subsurface morphological features of a Venusian lava flow, varying geoelectric models through RS data simulations.

This work was supported by the Italian Space Agency under Grant n. 2022-23-HH.0 'Attività scientifiche per il radar sounder di EnVision fase B1'

2. METHODOLOGY

In this work, the RS data simulations of different geoelectrical models of a Venusian lava flow measured with SRS parameters are performed by exploiting the Multi-layer Coherent RS Simulator (MCS) [11], which is a state-of-art ray-tracing based simulation technique. Planetary RS missions often rely on ray-tracing simulations due to their simplicity and ease of surface modeling. MCS employs the Stratton-Chu integral to calculate the total received electromagnetic field, using the Huygens' principle and Snell's law for field propagation. The target is modeled with multiple layers, each divided into planar facets, reducing computational resources and time. This approach allows for efficient large-scale simulations with various target assumptions and is significantly faster than numerical electromagnetic simulators.

Figure 1 provides a summary of the key steps in the considered workflow. The simulation methodology requires input parameters for both the SRS radar and the geoelectric model of the specific scenario under consideration. The geoelectric model is constructed by defining the geological and geophysical characteristics of the target, which are then transformed into the geometric and dielectric properties within the geoelectric model. The MCS-based simulation methodology generates a collection of simulated radargrams along with the respective clutter simulations, showcasing the diverse SRS radar responses for a Venusian lava flow scenario. This set of RS data generates a database of simulations, illustrating how the SRS radar responses vary with changes in the geological and geophysical characteristics across different input geoelectrical models. The assessment of SRS's capability to detect subsurface structures within the Venusian lava flow involves the analysis of the database of simulations. The subsurface response of the Venusian lava flow is analyzed by comparing the radargrams simulated for different parameter values. This evaluation entails comparing results while systematically varying one geoelectric parameter at a time. More in detail we consider: (i) **Clutter power analysis versus surface dielectric properties variation**, in which the interaction between the power distribution of the clutter (a possible masking source of subsurface responses) and changes in surface dielectric properties is studied by holding the thickness of the lava flow and the dielectric properties of the subsurface constant; (ii) **Subsurface dielectric properties variation**, in which the behavior of subsurface layer dielectric effects is analysed while keeping lava flow thickness and surface dielectric properties constant; (iii) **Loss tangent variation**, in which the effects of loss tangent variations applied to the entire model is investigated, while keeping lava flow thickness constant; (iv) **Lava flow thickness variation**, in which the subsurface responses is evaluated, keeping the surface and subsurface dielectric properties constant while varying lava flow thickness.

To analyze SRS detection capability via comparison of simulated data, we extract surface, clutter, and subsurface

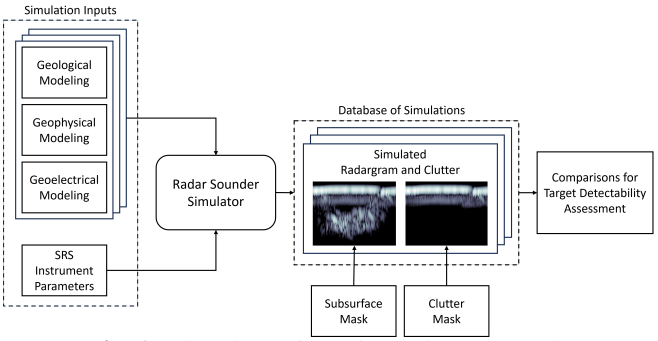

Fig. 1: Flowchart of the simulation approach.

power responses. Surface power response P_s is obtained from radargrams by selecting the maximum value of each simulated rangeline. Clutter power response P_c is derived from clutter simulation of the surface using a defined clutter influence area mask, which relies on the maximum clutter depth d_c:

$$d_c = \frac{ct}{2\sqrt{\epsilon_r}} \tag{1}$$

determined by surface dielectric properties ϵ_r and the time delay t between the first and last clutter return. Subsurface power response P_{ss} is acquired by defining a mask over the radar response influence of the subsurface, retrieved from the difference between simulated radargrams and corresponding clutter simulations.

For assessing the detection capabilities of SRS for subsurface structures within lava flows, it is considered that the power of the subsurface echo P_{ss} must be grater than the Radar Dynamic Range (RDR). The RDR is dependent on the sidelobe power level of the transmitted signal and is around $-55dB$. This value sets the minimum detectability level for subsurface echoes. This condition can be verified through the computation of the subsurface-to-surface ratio (SSR), computed as follows:

$$SSR = P_{ss} - P_s \tag{2}$$

where P_{ss} and P_s are the peak power values extracted from the subsurface mask and from the surface for each rangeline of the radargram, respectively. The probability of detecting subsurface echoes increases with the increase of the SSR.

To assess the impact of clutter as a masking source for the subsurface response of lava flow's structures, the Subsurface-to-Clutter Ratio (SCR) is computed. The SCR is defined as follows:

$$SCR = P_{ss} - P_c \tag{3}$$

where P_{ss} and P_c represent the peak power values extracted from the subsurface mask of the radargram and the clutter mask of the corresponding clutter simulation, respectively. As the SCR decreases, the probability of clutter masking the subsurface echoes increases. This provides a quantitative measure of the impact of clutter on the detectability of subsurface structures.

3. EXPERIMENTAL RESULTS

3.1. Simulation setup

To overcome the limited data available on Venus, the geological model of a lava flow can be obtained from other planetary bodies. This is reasonable as similar geomorphological processes occur in all celestial objects, even if with variations in scale and dielectric properties. Therefore, we chose to model a geological area of interest on Venus using similar features identified on Mars south of Alba Patera, the northern flow complex centered at $17.5°N$, $109°W$ [12]. Figure 2 shows the DEM obtained from the MOLA altimeter on the Mars Express mission and the retrieved binary mask separating the lava flow from the surrounding plains. Following an eruption,

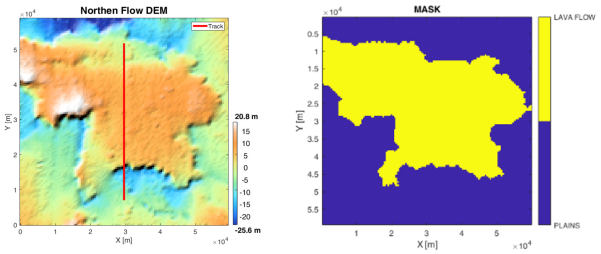

(a) (b)

Fig. 2: Venus lava flow model: a) surface DEM; and b) binary mask identifying the area of the lava flow and the plains.

the lava flow covers a portion of the terrain, inducing both structural and geological changes through surface heating. In our proposed model, we assume that the subsurface profile mirrors the surface profile. To explore the various possible scenarios, we have adjusted the maximum thickness of the entire lava flow area, considering values up to $400\ m$, which is the reported maximum in the Venus literature. [13]. Combining a range of dielectric and loss tangent parameters (shown in the Table 1) expected for volcanic regions on Venus, [12], [14], [15] geoelectric models are generated from four geological models that represents lava flows with diverse thicknesses. This involves assigning values to the lava flow surface, the surrounding plains area, and the subsurface of the lava flow.

Table 1: Venus lava flow parameters considered in the simulations.

Lava Flow Parameter	Range of values
Dielectric property [14, 15] (lava flow and plains areas)	[2.5, 4, 5, 7, 9]
Loss tangent [12]	[0.01, 0.06]
Maximum thickness [13] lava flow models	[40, 80, 200, 400] m

Table 2: SRS instrument parameters considered in the simulations.

SRS Instrument Parameter	Value
Central frequency	9 MHz
Bandwidth	5 MHz
PRF	400 Hz
Peak transmitted power	200 W
Sampling frequency	60 MHz
Spacecraft altitude	250 km
Footprint radius	7 km

The SRS parameters provided in the Table 2 are considered in the simulations. The experiments are executed by modeling the platform path with the track orientation aligned along the y-axis of the target model. Following the simulation process, a total of 1000 radargrams were generated by combining the parameters outlined in Table 1. Additionally, 50 corresponding clutter simulations were produced, resulting in the creation of a simulation database comprising 1050 simulations.

3.2. Results

This subsection presents the results derived from the comparative analysis of the simulated radargrams and the relative cluttergrams within the database. Given the morphological features of the simulated lava flow, the plain marginally influences the detection of the lava flow subsurface. However, due to space constraints, we report only the worst-case scenario in which the plain has dielectric properties equal to those of lava flow subsurface.

To provide a thorough understanding of the SRS detection capabilities, we present the SSR variation, under the aforementioned conditions, with the respect to the geolectrical and morphological features of the lava flow for loss tangent values of 0.01 and 0.06. Additionally, we report a comprehensive clutter analysis based on the variation of clutter power concerning the dielectric properties of the surface of both lava flow and plain, and its impact on masking the lava flow subsurface signal measured in terms of SCR.

Clutter power analysis versus surface dielectric properties variation: Higher dielectric values correlate with an increase in the peak power of the surface. Moreover they influence the clutter impact on the subsurface detection. However, as shown in figure 3, given the morphological structure of the simulated lava flow and the relative SRS trajectory, the choice of the dielectric properties of the plains has a marginal effect on the clutter power, with a maximum variation of about 2 dB. Let us consider the worst-case conditions for the subsurface detectability where $\epsilon_{SS} = \epsilon_P$ and lava flow thickness is equal to 40 and 80 m: we can observe in figure 4 how the SCR varies with respect to both the dielectric properties and the thickness

of the lava flow layers. By combining the received signal with the dielectric features, we can determine the maximum clutter depth equal to 100 m for $\epsilon_{LF} = 2.5$ and equal to 53 m for $\epsilon_{LF} = 9$ (illustrated in figure 4 by the light grey curve). In this context the subsurface signal is severely compromised by the presence of clutter only when the maximum thickness of the lava flow is 40 m. At 80 m, the presence of clutter decreases as the dielectric properties of the lava flow surface increase, and the SCR is more significantly influenced by the dielectric contrast.

Subsurface dielectric properties variation: Changes in subsurface dielectric properties significantly affect subsurface signal reflectivity. As shown in figure 5, by fixing the loss tangent value and the overall thickness of the lava flow model, an increased dielectric contrast between surface and subsurface enhances reflectivity at layer interfaces, thereby improving the detectability of the subsurface signature. Indeed, in the optimal detectability conditions with $loss_{tg} = 0.01$ and overall thickness of 200 m, the SSR varies between -11.20 dB and -19.47 dB for the highest and the lowest dielectric contrasts, respectively. However, increasing the overall thickness to a maximum of 400 m, the attenuation of the subsurface signal increases resulting in a power level eventually below the RDR with a decreased capability of detecting the subsurface contribution.

Loss tangent variation: An increase in the loss tangent results in greater attenuation of the radar signal, reducing both the maximum depth of subsurface detection and the strength of the reflected signal. From figure 5 a comparison of the variation of two of the expected Venusian's lava flow loss tangent values can be done by fixing the dielectric contrast between the surface and the surface and the overall thickness of the lava flow. The results of the computed SSR on the simulated database show a decrease when the loss tangent increases. The subsurface detection is better for materials with a low loss tangent, which allow for greater signal penetration.

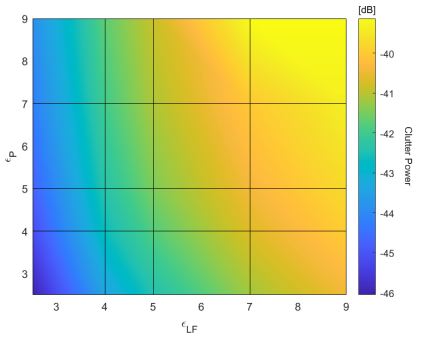

Fig. 3: Variation of clutter power with respect to the dielectric properties of the lava flow surface and surrounding plains. The grid intersections are combinations of the simulated dielectric properties.

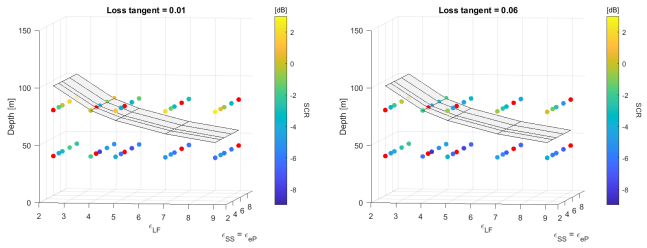

(a) (b)

Fig. 4: SCR variation of the simulated lava flow models with respect to the clutter maximum depth by fixing (a) $loss_{tg} = 0.01$ and (b) $loss_{tg} = 0.06$. The light grey grid is the clutter depth variation, while the points in red represent the simulated models with the non-detectable condition of $P_{SS} < RDR$.

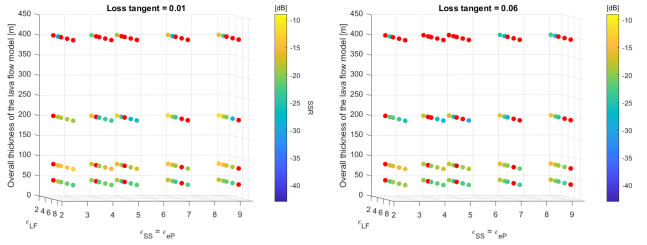

(a) (b)

Fig. 5: SSR variation of simulated lava flow models by fixing (a) $loss_{tg} = 0.01$ and (b) $loss_{tg} = 0.06$. The points in red represent the simulated models with the non-detectable condition of $P_{SS} < RDR$.

4. CONCLUSIONS

The assessment of the SRS capability to detect Venusian lava flows reveals favorable conditions for achieving the scientific objectives of the mission, considering the specified SRS parameters. The comparisons among simulated radargrams in the generated database provide quantitative indications on the boundary constraints for the detection. These conditions confirm that a greater dielectric contrast between the surface and subsurface layer of the lava flow substantially enhances detection capability. In the same way, lava flow formations characterized by higher loss tangent values can be better detected at a moderate depth as the attenuations can decrease the detection capability for large flow thickness. Clutter potentially masks signals from subsurface structures up to a maximum lava flow thickness (which depends on the surface DEM) of 100 m. However, signals characterized by a sufficiently high power are not completely obscured, allowing SRS to distinguish the subsurface contribution.

As future work, we plan to extend the study to various morphologies of Venusian lava flows and to quantify the extent of detectable subsurface under various conditions.

5. REFERENCES

[1] L. J. Porcello et al., "The apollo lunar sounder radar system," *Proceedings of the IEEE*, vol. 62, no. 6, pp. 769–783, 1974.

[2] T. Ono et al., "Instrumentation and observation target of the lunar radar sounder (lrs) experiment on-board the selene spacecraft," *Earth Planets and Space*, vol. 60, 04 2008.

[3] R. Croci et al., "The shallow radar (sharad) onboard the nasa mro mission," *Proceedings of the IEEE*, vol. 99, no. 5, pp. 794–807, May 2011.

[4] G. Picardi et al., "Marsis, a radar for the study of the martian subsurface in the mars express mission," *Memorie della Societa Astronomica Italiana Supplement*, vol. 11, pp. 15–25, 01 2007.

[5] S. Plaut et al., "Jupiter icy moons explorer (juice): Science objectives, mission and instruments," 01 2014.

[6] L. Bruzzone et al., "Rime: Radar for icy moon exploration," in *2013 IEEE International Geoscience and Remote Sensing Symposium - IGARSS*, July 2013, pp. 3907–3910.

[7] D. Blankenship et al., "REASON for Europa," in *42nd COSPAR Scientific Assembly*, July 2018, vol. 42, pp. B5.3–55–18.

[8] L. Bruzzone et al., "Envision mission to venus: Subsurface radar sounding," in *IGARSS 2020 - 2020 IEEE International Geoscience and Remote Sensing Symposium*, 2020, pp. 5960–5963.

[9] S. Thakur et al., "Venus subsurface targets: assessment of detectability using radar sounder simulations," Tech. Rep., Copernicus Meetings, 2020.

[10] S. Thakur et al., "Analysis of surface clutter for subsurface radar sounding on venus," in *IGARSS 2022-2022 IEEE International Geoscience and Remote Sensing Symposium*. IEEE, 2022, pp. 1340–1343.

[11] C. Gerekos et al., "A coherent multilayer simulator of radargrams acquired by radar sounder instruments," *IEEE Transactions on Geoscience and Remote Sensing*, vol. 56, no. 12, pp. 7388–7404, 2018.

[12] L. M. Carter et al., "Dielectric properties of lava flows west of ascraeus mons, mars," *Geophysical Research Letters*, vol. 36, no. 23, 2009.

[13] K. M. Roberts et al., "Mylitta fluctus, venus: Rift-related, centralized volcanism and the emplacement of large-volume flow units," *Journal of Geophysical Research: Planets*, vol. 97, no. E10, pp. 15991–16015, 1992.

[14] B. A. Campbell et al., "Analysis of volcanic surface morphology on venus from comparison of arecibo, magellan, and terrestrial airborne radar data," *Journal of Geophysical Research: Planets*, vol. 97, no. E10, pp. 16293–16314, 1992.

[15] N. V. Bondarenko et al., "Correlation of dielectric permittivity of volcanic units on venus with age," *Journal of Geophysical Research: Planets*, vol. 108, no. E2, 2003.